

Deep learning-based survival prediction of brain tumor patients using attention-guided 3D convolutional neural network with radiomics approach from multimodality magnetic resonance imaging

Moona Mazher¹  | Abdul Qayyum² | Domenec Puig¹ | Mohamed Abdel-Nasser³

¹Departament d'Enginyeria Informàtica i Matemàtiques, Universitat Rovira i Virgili, Tarragona, Spain

²National Heart and Lung Institute, Imperial College London, London, UK

³Electronics and Communication Engineering Section, Electrical Engineering Department, Aswan University, Aswan, Egypt

Correspondence

Moona Mazher, Departament d'Enginyeria Informàtica i Matemàtiques, Universitat Rovira i Virgili, 43007 Tarragona, Spain.
Email: moona.mazher@estudiants.urv.cat

Funding information

Spanish Government through Projects TED2021-130081B-C21, PDC2022-133383-I00, PID2019-105789RB-I00

Abstract

Automatic survival prediction of gliomas from brain magnetic resonance imaging (MRI) volumes is an essential step for a patient's prognosis analysis. Radiomics research delivers beneficial feature information from MRI imaging which is substantially required by clinicians and oncologists for predicting disease prognosis for precise surgical treatment and planning. In recent years, the success of deep learning has been vast in the field of medical imaging, and it shows state-of-the-art performance in applications like segmentation, classification, regression, and detection. Therefore, in this paper, we proposed a collective method using deep learning and radiomics techniques for the survival prediction of brain tumor patients. We first propose a hierarchical channel attention (HAM) module and a multi-scale-aware feature enhancement (MSAFE) to efficiently fuse adjacent hierarchical features in the proposed segmentation model. After segmentation, deep/latent features (LCNN) are extracted from the bottom layer of the proposed segmentation model. Later, we extracted selected radiomics features (histogram, location, and shape) using input images and segmented masks from the proposed segmentation model. Further, the 3D deep learning regressor has been trained for 3D regressor-based deep feature extraction. We proposed the method of overall survival prediction for the brain tumor patients by combining all the meaningful features including clinical features (age) that also favorably contribute to the survival days prediction for the glioma's patients. To predict the survival days for each patient, the selected features are trained to analyze the performance of various regression techniques like random forest (RF), decision tree (DT), and XGBoost. Our proposed combined feature-based method achieved the highest performance for survival days prediction over the state-of-the-art methods. We also perform extensive experiments to show the effectiveness of each feature extraction method. The experimental results infer that deep learning-based

This is an open access article under the terms of the [Creative Commons Attribution-NonCommercial-NoDerivs](https://creativecommons.org/licenses/by-nc-nd/4.0/) License, which permits use and distribution in any medium, provided the original work is properly cited, the use is non-commercial and no modifications or adaptations are made.

© 2023 The Authors. *International Journal of Imaging Systems and Technology* published by Wiley Periodicals LLC.

features along with radiomic features and clinical features are truly vital paradigms to estimate survival days.

KEYWORDS

brain tumor, brain tumor prognosis, deep learning, medical image processing, multimodal brain tumor, radiomics, segmentation, segmentation, survival prediction

1 | INTRODUCTION

Gliomas are the most common brain tumor disease developed from glial cells with the greatest mortality rate. There are 190 000 glioma cases annually occurring worldwide.¹ Approximately 12 months² is the average survival time of glioma patients and 24 months after surgical resection,³ roughly 90% of patients unluckily die due to this disease. For automatic survival prediction and treatment planning, automatic delineation, early detection, and volume estimation are important tasks in detecting gliomas. Due to the high variation of shape, appearance, and location of gliomas, it is a challenging task to localize and delineate the gliomas using conventional segmentation methods. Moreover, human experts need to closely monitor the manual segmentation annotation of tumor tissue which is a tedious and time-consuming task. Consequently, there is always a need for automatic, accurate, and faster methods for segmentation and survival rate prediction that could be helpful for the diagnosis and treatment of gliomas. The volume, shape, textural, and intensity extracted from radiographic images are known as radiomics.⁴

Radiomics includes numerous important disciplines, incorporating computer vision for quantitative feature extraction, radiology for imaging interpretation, and machine learning for classifier⁵ assessment and regression.⁶ Various radiomics-based models have been presented for survival prediction,⁷ and distant metastasis prediction.⁸ Shboul et al.⁹ proposed texture, area, volume, and Euler characteristics-based radiomics features from different intra-tumor parts. They achieved 0.519 accuracies in survival prediction tasks in brain tumor segmentation (BraTS) 2018 test data. Feng et al.¹⁰ proposed basic machine learning-based algorithms such as simple linear regressors using some volume, surface area, and directional gradient features for survival prediction. Their method was overfitted due to a small set of feature extraction and did not optimize well for survival prediction.

Chaddad et al.⁴ used a gradient boosting algorithm and random forest machine learning methods based on multi-scale texture features for survival prediction. Osman et al.¹¹ presented 147 sets of radiomics image features using three tumor subregions and used the Least

Absolute Shrinkage and Selection Operator (LASSO) regression model for survival prediction. Sun et al.¹² presented 4524 radiomic features from the segmented area of the tumor and used a decision tree machine learning model for survival prediction. Baid et al.¹³ proposed a gray-level co-occurrence matrix, shape features, and first-order statistics features, they used artificial neural network (ANN) model for survival prediction. Kim et al.¹⁴ introduced radiological features from MR images and used the LASSO model for survival days prediction. Weninger et al.¹⁵ proposed volume, distance, the center of the mass tumor, and age radiomics features using linear regression for survival prediction. Wang et al.¹⁶ proposed radiomics analysis software to extract 43 unique quantitative features and support vector machine (SVM) machine learning model used for survival prediction.

Recently, deep learning models achieved state-of-the-art performance in medical image analysis for regression, classification,¹⁷ segmentation,^{18,19} and detection application.²⁰ The deep learning-based models produced an excellent performance in recognizing objects and diagnosing diseases from medical images.^{21,22}

Khan et al.²³ proposed deep learning-based segmentation models to extract CNN features and combined hand-crafted features such as texture, histogram, volume, area, and run length. Banerjee et al.²⁴ presented a deep learning-based method for survival prediction using BraTs 2019 dataset. Their approach did not achieve better performance in the overall survival prediction task. Alain et al.²⁵ proposed a residual convolutional neural network segmentation model to extract volume, heterogeneity, rim width, and surface irregularity features from the segmented tumor.

Mubarak et al.²⁶ proposed a CNN model and extracted volume, heterogeneity, rim width, and surface irregularity from the segmented tumor. Further, they combined imaging and clinical features for survival prediction.

Huang et al.²⁷ proposed a non-local module-based VNet model to segment brain tumors. Further, they have extracted CNN-based deep features and imaging radiomics features. They tested their method using the BraTS 2020 dataset and achieved a 79% dice score for segmentation and 311.5 RMSE values in survival days prediction.

Sveinn Pálsson et al.²⁸ proposed imaging features and used a machine-learning model for survival prediction.

They tested their method on the BRaTs 2020 dataset and achieved a 0.61 C score between predicted and ground-truth survival days.

CNN-based features are robust and automatically extracted from images without manual intervention. In contrast, the traditional methods used handcrafted features like radiomics, and the data-driven-based approach extracted imaging features automatically like for complex segmentation tasks. It validated from the literature that high-level features like shapes extract global semantic information and low-level features like contours extract details of spatial structural information. Hence, the features from different neural network layers are used to combine effective features from previous cascaded layers intuitively.

In this article, we proposed an attention-based convolutional neural network (CNN). We propose a multi-scale-aware feature enhancement (MSAFE) module that adjusts the receptive fields dynamically to produce efficient features effectively, thus improving the feature representation capability of the network. Later, we extracted the deep/latent CNN features (LCNN) from the trained proposed CNN model along with the specifically selected radiomics feature (histogram, location, and shape) using input images and segmented masks. These features enhanced the performance of our proposed solution. A better segmentation mask produced better radiomics features that boost the performance of the proposed solution for survival days prediction.

Furthermore, we proposed our final method of overall survival prediction by combining all the meaningful features including clinical features (age) that contribute to the number of days of survival left for the patient. To predict the survival days for each patient, the selected features are trained to analyze the performance of various regression techniques. Details about how the features are selected and various experiments that are run to find the best regression technique have been discussed in the next sections. To assess the generalization capability of our proposed solution is also given on the Head & Neck Tumor dataset (HECTOR2021).

2 | PROPOSED TUMOR SEGMENTATION MODEL

This section presents the dataset and architectural details of the proposed deep learning models and radiomics features for BraTS and survival days prediction.

2.1 | Dataset

BraTS has been published since 2012 at the Medical Image Computing and Computer-Assisted Intervention (MICCAI)

conference.²⁹ The overall survival prediction task is included from 2017 until 2020 BraTS challenges. The total number of subjects in the training set of BraTS 2020 with their masks is 369 and the dataset was taken from different institutions using different scanners and clinical protocols.²⁹

This dataset is divided into two sets, one for training and one for testing the proposed model. A ratio of 80:20 is used for training and testing set division. The total training set holds 295 subjects, and the testing set holds 74 subjects. Each subject has nifti volumes for Flair, T1, T1CE, and T2 MRI modalities of size $240 \times 240 \times 155$. There are three classes of tumor given in the ground-truth (GT) masks including enhancing tumor (ET) (labeled as class-4 in GT), peritumoral edema (ED) (labeled as class-2 in GT), and non-enhancing tumor/ necrotic tumor (NCR) (labeled as class-1 in GT). In our experiment, all four MRI modalities are stacked for BraTS using the proposed model. Further, the resection status, age, and survival in days were also provided for overall survival prediction. Figure 1 shows the Flair, T2, T1, T1CE, and the corresponding segmentation GT of a subject from the BraTS dataset (2020).

Here, the green color in the GT segmentation represents the ET class, the yellow color stands for ED, and the red color holds for the NCR tumor class. The segmentation labels in this dataset are enhancing tumor region (ET), tumor core (TC), and whole tumor (WT).

2.2 | Proposed method for survival prediction

The training and validation datasets use stacked images of four MRI modalities. A 3D deep learning segmentation model has been proposed to segment brain tumors and is further used in survival prediction. The deep features (LCNN) are extracted from the bottom layer of the encoder from trained segmentation masks. Furthermore, the input volume and predicted segmentation masks have been used to extract radiomics features. We also have used some feature selection techniques to select the best radiomics and LCNN for survival days prediction.

The variance-based feature selection technique is used to select the best features. Moreover, the features are normalized and fed into traditional machine learning-based classifiers such as random forest, gradient boosting, etc. Furthermore, the 3D deep learning-based CNN regressor (3DReg) model has been trained for deep feature selection. Thereafter, a feature selection is also applied to select the useful 3DReg features. Different performance metrics have been used for survival days prediction. The overall schematic diagram of the proposed methodology is given in Figure 2.

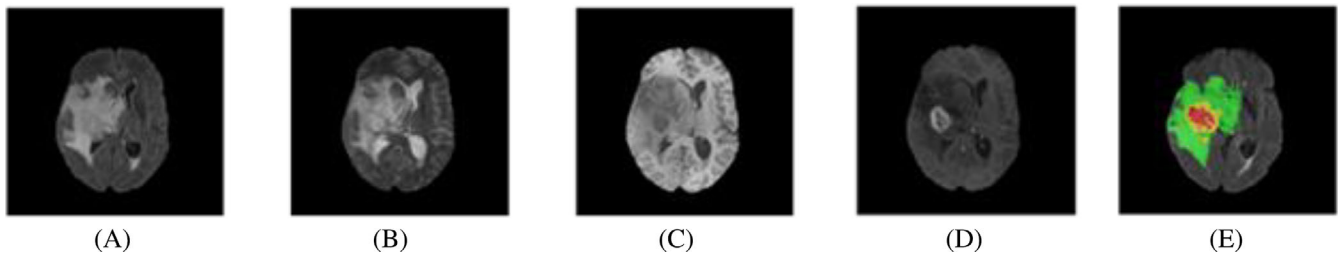


FIGURE 1 The four MRI modalities were used in this study. (A) shows the Flair image, (B) shows the T2 image, (C) shows the T1 image, (D) shows the T1CE image, and (E) shows the ground-truth mask.

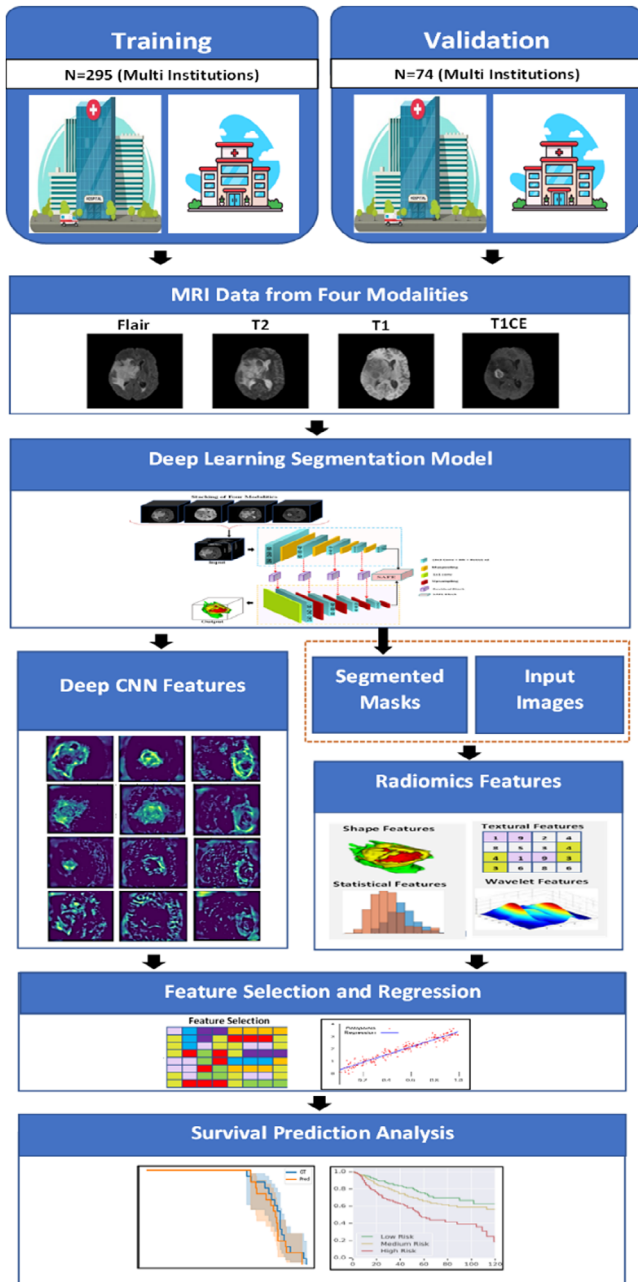


FIGURE 2 Overall proposed technique for survival days prediction based on deep and non-deep learning feature extraction methods.

The detailed description of each module is explained in the following subsections.

2.3 | The proposed segmentation framework

Figure 3 illustrates the proposed CNN model for BraTS, which includes encoder and decoder networks. Four MRI modalities (T1, T1CE, T2, and Flair) have been stacked as the input and predicted masks are produced for each tumor class (enhancing, non-enhancing/necrotic, and peritumoral edema) highlighting the tumor regions. The convolutional block consists of 3D convolutional layers with Batch-Normalization and ReLU activation functions to extract the different feature maps from each block on the encoder side. The 3D max-pooling layer has been used to reduce the input image spatial size. In the encoder block, the spatial input size is reduced with increasing the number of layers, while on the decoder side, the input image spatial resolution is recovered via a 3D upsampling layer using a bilinear upsampling method. Each MRI modality has a $160 \times 160 \times 80$ input size. The number of input channels is 4 (stacked four modalities of input dataset). The number of feature maps for each encoder block is 32, 64, 128, and 256. The kernel size of $3 \times 3 \times 3$ is used for each Conv layer in the encoder and decoder blocks. The kernel size $2 \times 2 \times 2$ for the 3DmaxPool layer is used to downsample the spatial resolution on the encoder side. The transpose3D convolutional layer with $2 \times 2 \times 2$ kernel size with stride 2 is used to upsample each decoder size.

We introduced two special modules for our 3D CNN model. First, we have proposed a 3D hierarchical attention module (HAM) for the proposed BraTS model as shown in Figure 4. The HAM block has been used after each encoder block to concatenate with their corresponding decoder blocks. The 1×1 convolutional layer with softmax function has been used at the end of the proposed model to generate the final output.

FIGURE 3 Diagram of the proposed model with the proposed MSAFE module and the HAM block.

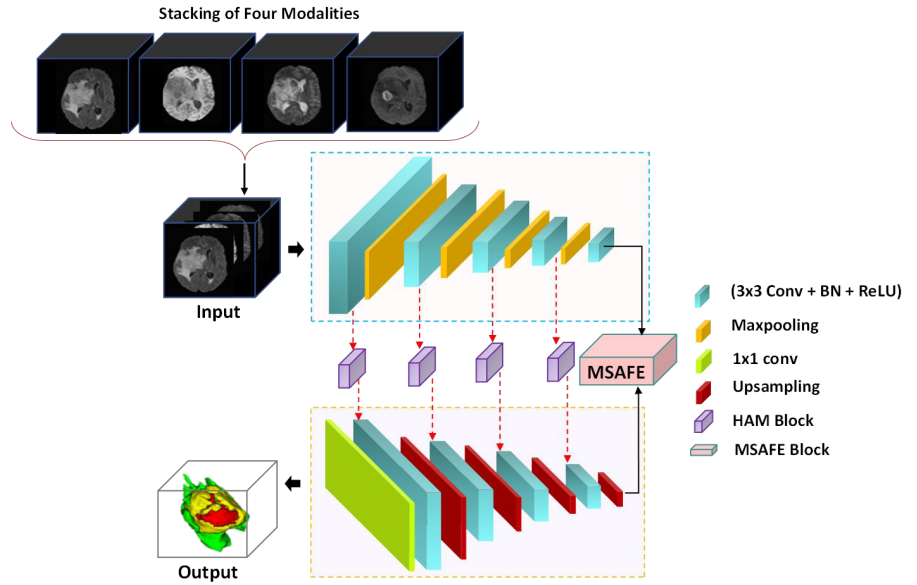
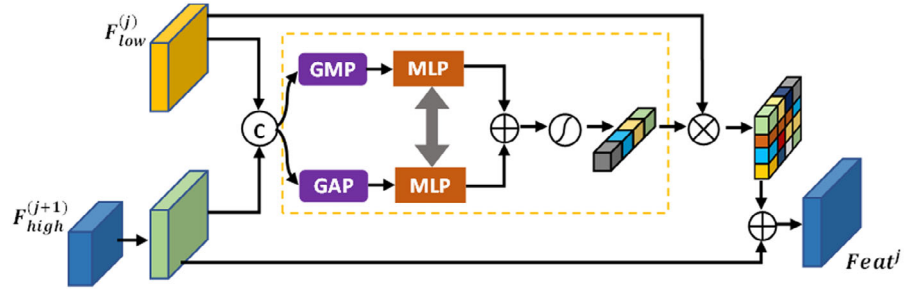


FIGURE 4 Schematic diagram of hierarchical attention module (HAM).



We add the reweighted low-level features to the high-level features to yield the result $Feat^j$.

The mathematical representation of the proposed module is given below:

$$Feat_C^j = Concat\left(F_{low}^{(j)}, upsample\left(F_{high}^{(j+1)}\right)\right) \quad (1)$$

$$Feat^j = sigmoid\left\{L_{mlp}\left(L_{gap}\left(Feat_C^j\right)\right) + L_{mlp}\left(L_{gmp}\left(Feat_C^j\right)\right)\right\} \otimes F_{low}^{(j)} + F_{high}^{(j+1)} \quad (2)$$

where $Concat$ represents the concatenation operation, L_{mlp} denoted as MLP operator, L_{gap} denoted the global average pooling, L_{gmp} represents the global max pooling, and \otimes represents elementwise multiplication. The proposed module is used to progressively guide the fusion between high-level and low-level features that could help suppress irrelevant background noise and preserve more semantic information.

The proposed HAM module is used to progressively guide the fusion between high-level and low-level features that could help suppress irrelevant background noise and

preserve more semantic information. High- and low-level features from the encoder and decoder have rich semantic and spatial information that would be suitable for accurate segmentation. We designed an attention module with weighting vectors and used a channel attention module to capture rich semantic information from low-level features and high spatial information from high-level features. The features are concatenated between low-level and upsamples of the high-level features. The channel attention coefficient with sigmoid is used with multi-layer perceptron (MLP) and pooling layers to preserve relevant features as shown in Figure 4.

Second, we propose a multi-scale-aware feature enhancement (MSAFE) module. We embed the MSAFE module at the bottom of the framework which makes the model capable of extracting hidden multi-scale contextual information as well as able to aggregate multi-scale features efficiently. To obtain a more abundant feature map consisting of various receptive fields, we applied dilated convolutions with different dilation rates to all four parallel groups. As a result, the proposed network can extract adequately precise features at different scales. The detailed structure configuration of the MSAFE module is shown in Figure 5.

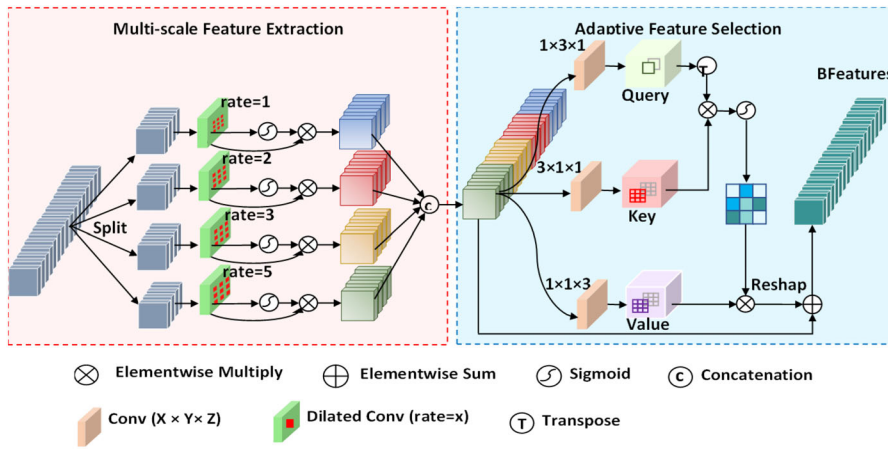


FIGURE 5 Multi-scale aware feature enhancement (MSAFE) module for brain tumor segmentation.

$$fm_i = \text{sigmoid}(D_c^{\text{rate}_i}(f_i)) \otimes D_c^{\text{rate}_i}(f_i) \quad (3)$$

$$HF = \text{Concat}(fm_1, fm_2, fm_3, fm_4) \quad (4)$$

where, $D_c^{\text{rate}_i}$ represents the dilated convolution layer with a dilated rate of rate_i ($r_1 = 1$, $r_2 = 2$, $r_3 = 3$, and $r_4 = 4$)

Finally, these hierarchical features HF are concatenated and delivered to the adaptive feature aggregation component to further model the importance of each feature.

The feature obtained from three views (sagittal, coronal, and axial) is passed to three Conv layers with BN and ReLU using different kernel sizes such as $3 \times 1 \times 1$, $1 \times 3 \times 1$, and $1 \times 1 \times 3$ in each convolutional layers to produced three feature maps. The activation maps from Q, K, and V are passed to the softmax layer. The importance of each feature is performed and these multi-scale feature maps to get the output of the proposed module are shown in Equation (5)

$$\text{BFeatures} = HF + \text{softmax}(Query^T \otimes Key) \otimes Value \quad (5)$$

where \otimes represents matrix multiplication and BFeatures represents bottom feature maps. Adopting the proposed module at the bottom layer after the last layer of the encoder can enhance the capability of the proposed model.

2.4 | Radiomics feature and imaging feature selection for survival prediction

In this work, we have extracted different multi-scale features from input MRI 3D volumes and segmented

tumor masks. The radiomics features are categorized as volume features, intensity-based features, and Geometrical features. The intensity-based features are Kurtosis, Entropy, and Histogram. The Geometrical features are Length and coordinates, First axis, Second axis, Third axis, Centroid coordinates, Eigenvalues, Equatorial eccentricity, and Meridional eccentricity. The further textural radiomics feature extracted from 3D MRI modalities input volume are (1) first-order statistics/statistical features (FOS/SF), gray-level co-occurrence matrix (GLCM/SGLDM), gray-level difference statistics (GLDS), neighborhood gray-tone-difference matrix (NGTDM), statistical feature matrix (SFM), Laws texture energy measures (LTE/TEM), fractal dimension texture analysis (FDTA), gray-level run length matrix (GLRLM), Fourier power spectrum (FPS), gray-level size zone matrix (GLSZM), higher order spectra (HOS), and local binary pattern (LPB).³⁰ These radiomics features approach is shown in Figure 6.

2.5 | Deep features extracted from the bottom layers of the segmentation model

Deep CNN features (LCNN) were extracted from the bottom layer of the trained encoder of the proposed segmentation model shown in Figure 3. The extracted feature vector has a 1×256 dimension extracted for each input 3D volume from the trained segmentation model. The performance of deep features is then analyzed using classical machine learning models.

FIGURE 6 The radiomics features extraction from deep learning segmentation masks for survival rate prediction.

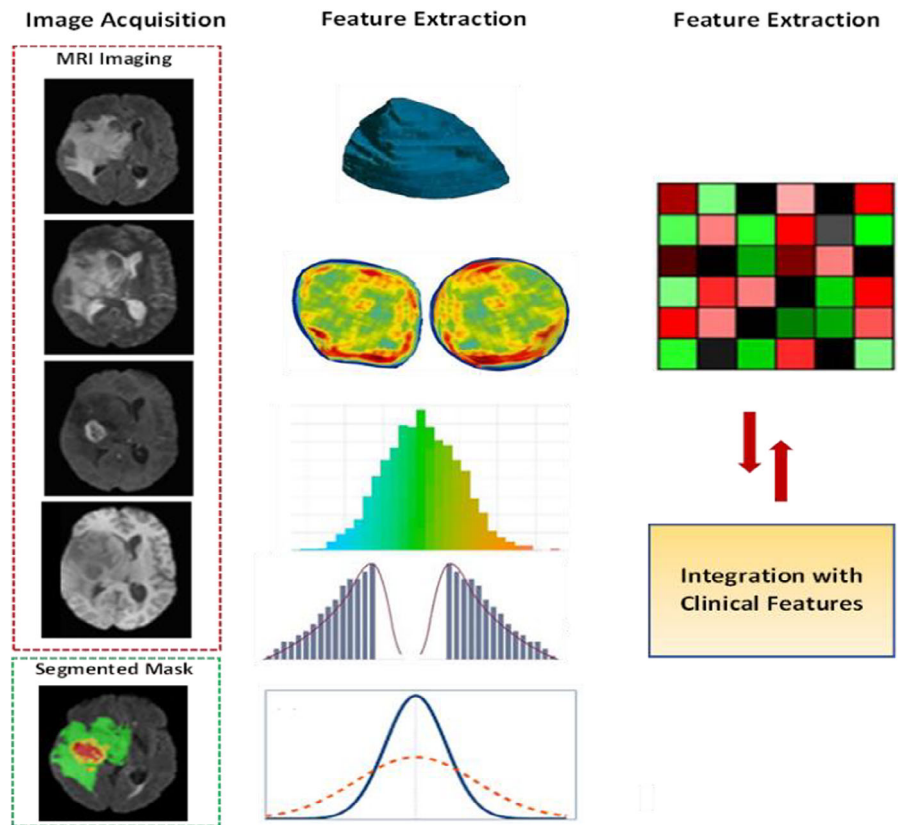
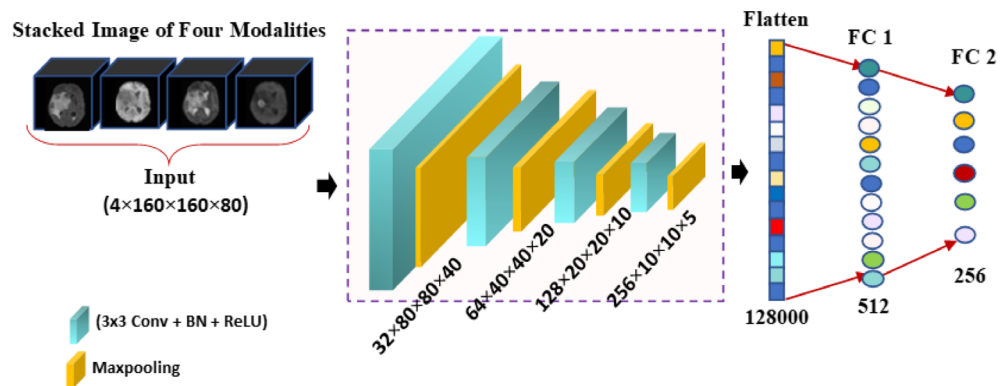


FIGURE 7 The proposed 3D deep learning regressor for survival days prediction using a brain tumor dataset.



2.6 | 3D deep regressor model

We have built a 3D regressor model based on the 3D convolutional, 3D Batch-Norm, and 3D ReLU layers. These three Layers (3DConv-BN-ReLU) formed one block. The proposed 3D-CNN network is a combination of these repeated layers followed by max pooling layers. After each convolution layer with the filter size of $3 \times 3 \times 3$, there is a max-pooling layer of size $2 \times 2 \times 2$. The 3D max-pooling layer is inserted after each block to downsample the spatial resolution of input feature maps. The first convolutional layer has a filter size of 16, and the number of filters in every next block is doubled to gain a rich feature vector of images. The number of feature maps increased by 32, 64, 128, and 256, and spatial resolution decreased by 160, 80, 40, 20, and

15. One flattened layer and two fully connected layers have been used to get the final feature output. Like the LCNN feature vectors, a total of 1×256 size of feature vector has been extracted for each input 3D volume. The proposed model is shown in Figure 7. L1 loss function has been used to compute the loss between predicted and ground-truth survival days. All model layers have been optimized from scratch using PyTorch.

2.7 | Regressor models for survival days prediction

The various regression models are used for survival days prediction. From experimental evaluation, the four

regression models random forest (RF),³¹ regression trees (RT), linear regression (LR), and extreme gradient boosting (XGB)³¹ produced acceptable performance. All regressors have been implemented using the sci-kit-learn tool with default setting (https://scikitlearn.org/stable/supervised_learning.html#supervised-learning).

2.8 | Loss function

The Combo loss function proposed by Taghanaki et al.³¹ has been used for the optimization and training of the proposed segmentation models. The loss function is defined as:

$$L = \alpha \left(-\frac{1}{N} \sum_{i=1}^N \beta(t_i - \ln p_i) + (1 - \beta)[(1 - t_i) \ln(1 - p_i)] \right) - (1 - \alpha) \sum_{i=1}^K \left(\frac{2 \sum_{i=1}^N p_i t_i + S}{\sum_{i=1}^N p_i + \sum_{i=1}^N t_i + S} \right) \quad (6)$$

where t_i represented target labels, p_i denoted as prediction mask, $\alpha, \beta \in [0, 1]$ and S are used as hyperparameters. All models are trained using Adam optimizer with a learning rate of 0.000116, $\rho = 0.95$, $\epsilon = 1e - 8$, and $decay = 0$. Experimentally, we found that $\alpha = 0.5$. We tried different β values with all used BraTS datasets, finding that $\beta = 0.5$ is the best value for our proposed model. For the survival prediction task, we have chosen root mean squared error (RMSE) as the evaluation indicator. The RMSE is shown in Equation (7).

$$RMSE = \sqrt{\frac{\sum_{i=1}^n (X_{obs,i} - X_{pre,i})^2}{n}} \quad (7)$$

where i represents the single case, n is denoted as the total number of cases, X_{obs} represents the true survival period of the case, and X_{pre} is denoted as a survival period predicted by the model.

Using the Adam optimizer, the proposed 3D segmentation model is optimized at the learning rate of 0.0001. The prediction mask generated by the proposed model has been resampled to have the same size and spacing as the original image and copies all the meta-data, including origin, direction, and orientation. The proposed models have been developed in the PyTorch library and trained from scratch. An NVIDIA GTX 3070 GPU having 12GM memory is used for the training and optimization of the proposed model.

3 | EXPERIMENTAL RESULTS AND DISCUSSION

This section covers in detail the results and their discussion on our proposed survival prediction techniques for brain tumor patients.

3.1 | Results

We described various feature extraction techniques and utilized multiple regression models for survival days prediction using the BraTS 2020 medical imaging dataset.

We have compared our proposed model with base UNet and ResNet-based UNet models. The base UNet is a simple encoder and decoder-based model and RUNet is the ResUNet base model. The 3D HAM modules are inserted in each decoder side of the base UNet. The dice scores coefficients (DSCs) and Hausdorff distance (HD) of the proposed model as well as RUNet and UNet models when segmenting the three brain tumor sub-regions (i.e., ET, WT, and TC) are shown in Table 1. The higher DSCs as well as the lower the HD in segmentation means elevated model performance.

TABLE 1 The performance comparison of proposed and existing deep learning models for brain tumor segmentation (BraTS).

Models	DSCs			HD		
	ET	TC	WT	ET	TC	WT
Proposed Model	0.883 ± 0.134	0.891 ± 0.178	0.902 ± 0.138	4.18 ± 0.822	3.62 ± 0.689	2.89 ± 0.253
RUNet	0.868 ± 0.145	0.872 ± 0.334	0.886 ± 0.138	6.33 ± 0.995	5.45 ± 0.887	4.35 ± 0.911
UNet	0.838 ± 0.1341	0.864 ± 0.874	0.874 ± 0.138	8.78 ± 0.989	7.90 ± 0.945	3.88 ± 0.673
Shah et al. ³²	--	--	0.90	--	--	--

Note: Bold value represents best scores.

TABLE 2 The performance comparison of different regression methods for survival days prediction.

Algorithm	3D regressor features	Clinical features	Latent 3D CNN features	Radiomics + clinical features	Combined features
RF	0.49	0.56	0.59	0.61	0.63
XGBR	0.54	0.56	0.6	0.57	0.62
DTR	0.51	0.55	0.57	0.56	0.61
GBR	0.53	0.53	0.53	0.55	0.6
ETR	0.55	0.51	0.58	0.53	0.62
BR	0.54	0.54	0.52	0.56	0.59

Note: Bold value represents best scores.

Table 1 shows that the base UNet model achieved the dice score and HD scores of 0.83, 0.86, and 0.87 and 8.78, 7.90, and 3.88 for ET, TC, and WT which are less than the achieved scores among all models. Similarly, the RUNet in comparison achieved fewer dice and high HD scores to its enhanced version of the proposed model. Therefore, the proposed model benefiting from the proposed MSAFE module and additional HAM blocks reached the ultimate performance scores by generating the highest dice score and smallest Hausdorff distance (HD) scores. It reveals that our proposed segmentation model outperforms the baseline UNet model and the other two comparison models on BraTS tasks. The higher segmentation performance scores are key to better survival predictions as they produce good-quality prediction masks.

For performance analysis, various machine learning regressors have been trained for survival predictions as shown in Table 2, and the performance is given in c-index. The random forest regressor produced a better performance as compared to other regressor models like decision tree (DTR), X-Gradient Boosting (XGBR), Gradient Bagging Regressor (GBR), extended Tree Regressor (ETR), Bagging Regressor (BR), etc.

Table 3 displays the results of the random forest model for the proposed feature extraction techniques in comparison with state-of-the-art methods in terms of the c-index. It is seen that when the radiomics features are combined with the clinical feature (Age), it achieves a state-of-the-art performance score. It could be because combining many features into a single feature led to generalizability that is derived via integrated inference skills shared across numerous feature sets.

Further, we estimated the RMSE scores for our proposed feature extraction methods using random forest regressor results and drew a performance comparison with existing state-of-the-art survival prediction methods as shown in Table 4. The proposed combined feature solution produced the lowest RMSE values as compared to state-of-the-art methods.

TABLE 3 C-index-based performance measured for survival days prediction.

Algorithms	C-index
3D Deep Regressor (3Dreg)	0.49
Clinical	0.56
Radiomics	0.57
3D Deep CNN Features (LCNN)	0.59
Radiomics + Clinical (RDCL)	0.61
Clinical + Radiomics + 3D Latent CNN + 3D Deep Regressor	0.63
²⁸ (Hd95 + Clinical + CoM + CEV)	0.61

Note: Bold value represents best scores.

3.2 | Performance analysis of the proposed model

The Kaplan–Meier curves based on ground-truth and predicted survival days using proposed feature extraction techniques are shown in Figure 8. We have used a random forest regressor to predict survival days using clinical, radiomics, and latent CNN features from the proposed segmentation model and deep CNN features from the trained 3D regressor. The curves show survival days prediction based on combined extracted features with random forest algorithms produced more accurately as compared to individual feature techniques for survival days prediction.

Figure 8A shows the survival days prediction curve with ground-truth survival days using combined features (clinical, radiomics, deep features). The random forest machine learning model based on radiomics features shows better performance after the combined feature approach is shown in Figure 8B. Figure 8C shows results based on latent deep 3D CNN features using random forest. The 3D Regressor model using a random forest is shown in Figure 8D. The combined feature approach produced better performance and predicted curves are very

	Method	MAE	RMSE
Existing method ²⁸	CNN+ Radiology+ Clinical	240.05	316.31
	Radiology+ Clinical	284.54	392.51
	CNN (RF)	284.13	378.85
	CNN (DL)	269.37	358.92
Proposed method	3D Deep Regressor (3DReg)	300.10	400.11
	Clinical	290.70	390.10
	3D Deep CNN (LCNN)	255.66	377.89
	Radiomics	247.56	321.23
	Combined + Clinical	243.99	310.11

TABLE 4 Performance of proposed and existing methods for survival days prediction.

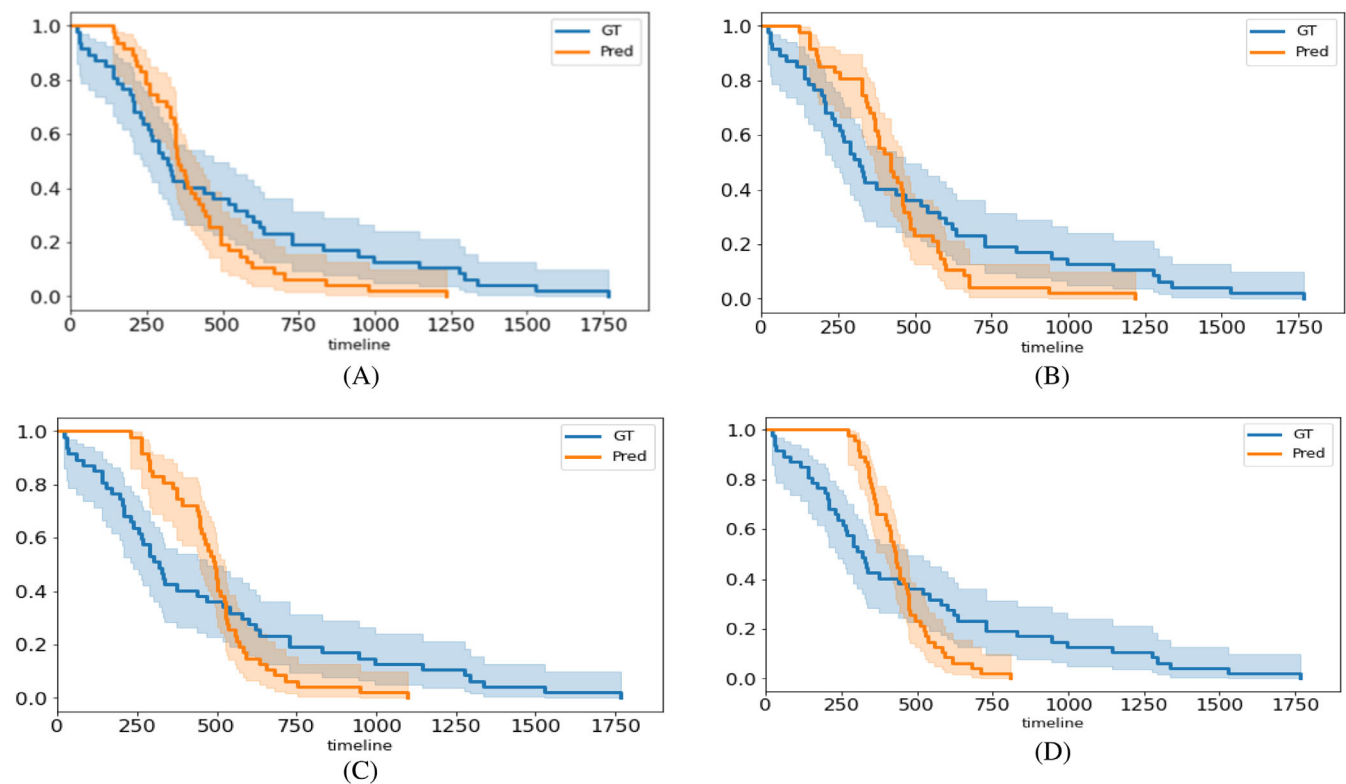


FIGURE 8 Kaplan–Meier plots of the (A) combined features radiomics, (B) radiomics features using RF classifier, (C) 3D deep extracted from segmentation model features with RF, (D) 3D deep learning regressor.

close to the target curves in terms of survival days as compared to individual-based features. Therefore, the curves produced by the proposed models validated the effectiveness of the survival days prediction method based on combined deep learning-based and radiomics features along with the clinical feature.

To investigate agreement between algorithm-generated and manually determined survival days, we used a Bland–Altman plot, which graphs the mean difference of measured survival versus manual survival days and constructs limits of agreement. Bland Altman represents the distribution of survival days output for clinical,

radiomics, deep learning features, and deep learning 3D regressor features. Bland Altman's plot shows the agreement between predicted and ground-truth survival days. Figure 9A based on the combined feature extraction approach represented the most agreement of predicted and ground-truth survival days as compared to other bland Altman plots. Similarly, the other plots are based on radiomics, and deep features are shown in Figure 9B–D.

We also validated our proposed model-based features using some statistical models such as *t*-tests. A *t*-test could be used to differentiate the difference between two

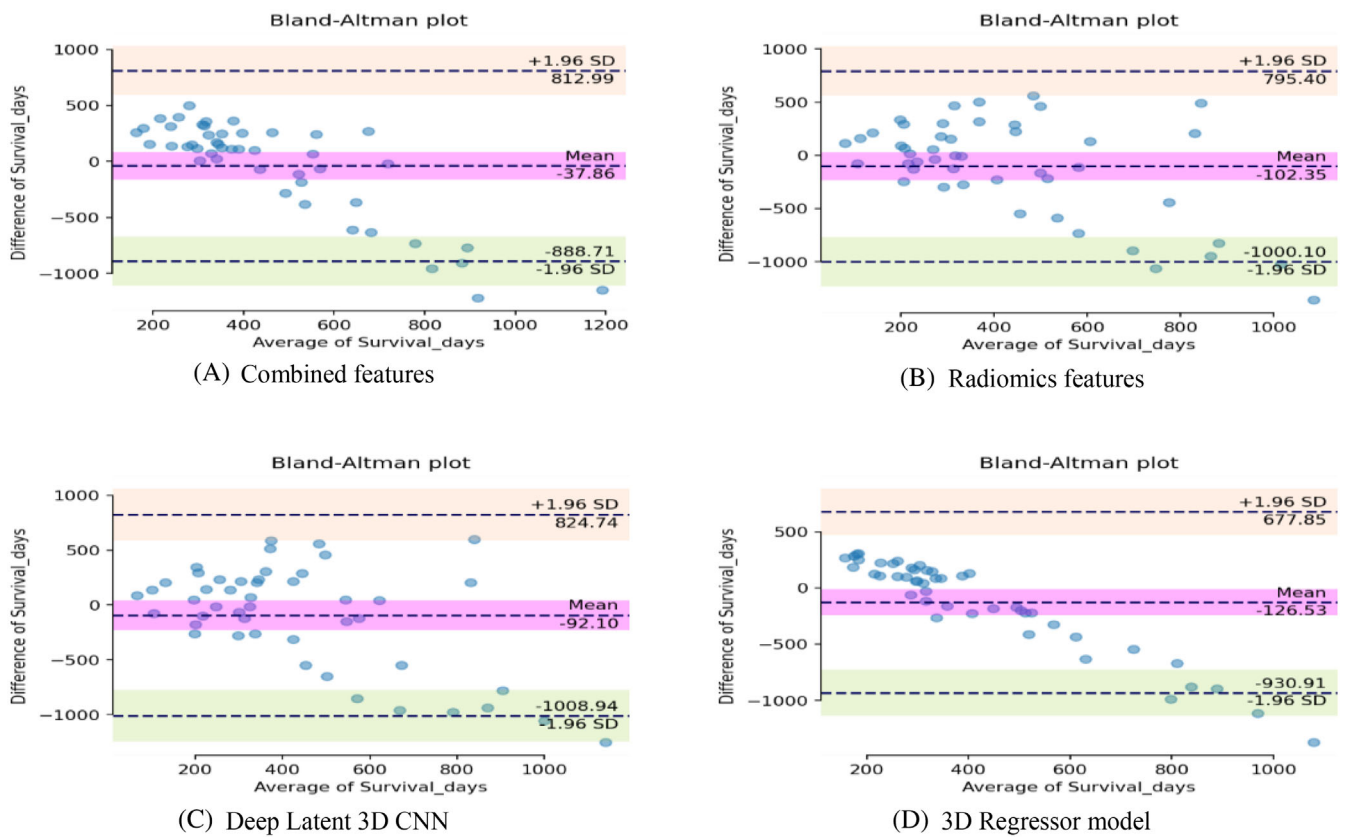


FIGURE 9 Bland Altman plot between predicted survival days and ground-truth survival days. (A) Combined (B) Radiomics + Clinical (C) Latent 3D CNN (D) 3D Regressor.

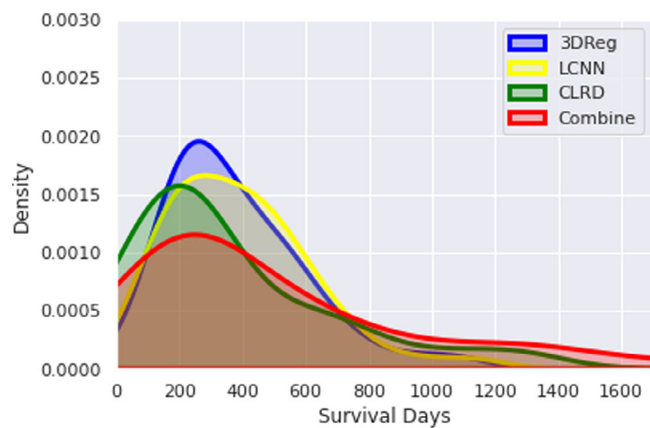


FIGURE 10 Density plots of the survival days prediction for the extracted features from 3D Regressor (3DReg), latent 3D CNN (LCNN), Radiomics + Clinical (CLRD), and their combined features (Combine).

or more groups. A lower p -value less than 0.005 shows that features have some statistical differences and a p -value greater than 0.005 shows that no difference between features that further was used in decision making.

Figure 10 shows the density plot for all survival prediction methods. Firstly, the distribution of the predicted survival days using combined features from all extracted feature techniques is significantly different from their separate outcomes. Similarly, the distribution score of predicted survival days with the combined feature approach is greater than their separate execution methods. However, prediction distributions of the 3D regressor distributions and latent 3D CNN techniques have larger standard deviations and more shift toward left as compared to the distribution of the Radiomics + Clinical feature approach.

The proposed combined feature solution is always shifted toward the higher values on the right as shown in Figure 11. The SHAP explainability method (SHapley Additive exPlanations)³³ has been used to measure the importance of deep CNN and radiomics features.^{34,35} The red color shows the high features and the blue color presents the low feature values.

Figure 11A,B shows the radiomics and deep features importance. It was shown that the skew, skew difference, and kurtosis achieved higher feature importance than the other features. We can say that the skew and kurtosis achieved higher feature importance as compared to other

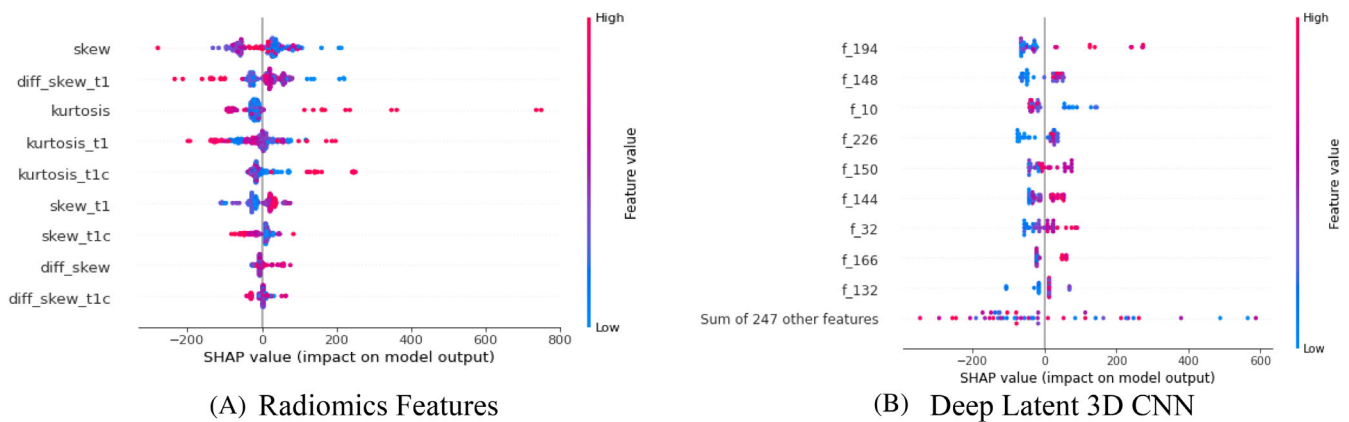


FIGURE 11 Radiomics feature importance for survival prediction. The red color presented high and the blue color presented low features in the prediction of the model (A) radiomics feature generation, (B) Deep Latent 3D CNN.

radiomics features. Out of 256 extracted features from the deep CNN method which produced the highest feature importance as compared to others are shown in Figure 11B.

3.3 | Generalization capability analysis

To see the generalization capability of our proposed solution for survival days prediction, we used the Hecktor2021 dataset.

I. Dataset: The head and neck tumor dataset proposed in MICCAI2021 has been used to validate our proposed solution. It consisted of 224 total training patients and 101 total tests acquired from 5 different centers. A detailed description of the dataset can be found.^{36–38}

II. Results: To estimate the number of survival days, we considered four previously mentioned feature extraction methods for the internal validation dataset: including clinical, CT/PET with radiomics, 3D deep segmentation-based features, and 3D regressor characteristics.

Results showed that the combined feature set (radiomics, clinical, and deep) gave the best performance when compared to the method using separate features. The combined features extraction strategy yields the best results for the RF model, as shown in Table 5 in terms of the c-index.

We compare the performance of our given method in terms of c-index with existing methods for survival days prediction using the HECTOR dataset as shown in Table 6. It is observed that our proposed combined feature approach outperformed the other state-of-the-art methods by yielding a c-index score of 0.84.

TABLE 5 The various regressor models for survival prediction in terms of C-index.

Algorithms	C-index
Clinical features	0.692
Deep segmentation features (LCNN)	0.788
Radiomics features (RD)	0.757
Deep 3D regressor features (3DReg)	0.794
Combined (Clinical + RD + LCNN + 3DReg) features	0.845

Note: Bold value represents best scores.

TABLE 6 Performance comparison with state-of-the-art methods.

Algorithms	C-index
Proposed method	0.84
Bourigault, E. et al. ³³	0.82
Muller, A. V. J. et al. ³⁴	0.59
Starke, S., et al. ³⁵	0.47

The diagnosis of squamous cell carcinoma requires the discovery of malignancy and the evaluation of prognostic outcomes. Effective detection may aid in better decision-making. Even if the segmentation and quantitative analysis of head and neck cancer is a notably complex task, the performance of the proposed framework is sufficient to be considered for automated diagnosis and survival rate prediction.

3.4 | Discussion

In this paper, we have trained a 3D segmentation model with different proposed modules to first segment the

tumor regions and generate the predicted masks. The proposed model yielded the best scores for DSCs and HD as the proposed MSAFE module in the segmentation model achieved better feature maps based on parallel dilated convolutional layers with different dilation rates by focusing different receptive fields. The proposed block extracts feature information dynamically based on different spatial scales and covered situations where brain tumors widely vary the size and shape.

Later, the input 3D volumes and segmented masks are passed for the radiomics feature extraction and selection. Also, we extracted the latent CNN features from the last encoder block of the trained segmentation model. Furthermore, we trained a 3D deep learning-based regressor model and extracted deep features from the last layer of the trained regressor model to predict survival days. We also used clinical features such as age and resection time provided in BraTS 2020 training data to train the random forest and other machine learning regressors.

Interestingly, adding a clinical training set did not significantly alter the results, which implies that the gap may be explained by clinical characteristics that are more pertinent when combined with different feature concatenation-based models. Contrary to most of the previous research on medical image diagnosis, in which clinical features play a significant role in prediction and diagnosis, we have discovered the fascinating fact that clinical features do not much contribute to performance improvement, indicating that most of the data is based on images. The geometric feature based on intensity, geometry, and location contributed more to predicting the survival days prediction. This study validated that the smaller the shape of the tumor produced, the higher overall survival and the immediacy of the tumor to the center of the brain achieved lesser performance for overall survival. The radiomics using images and masks produced higher explainable features for survival days prediction. Kurtosis and skewness achieved overall better performance and played a better role in predicting the overall survival days shown in the explainable feature plots. The performance of latent CNN deep learning-based features is almost comparable to the radiomics survival days prediction by observing the c-index scores.

The overall performance of the 3D deep learning regressor is not good as compared to radiomics and LCNN feature results. A deep learning-based regression model needs more input data for training, and we have used only 295 input samples. Therefore, it is observed we need more data to fully obtain the robustness in the results based on a 3D CNN-based regressor. Radiomics-

based features may have better interpretable advantages and generally more robust results can be obtained as compared to deep learning-based features.

However, our main objective is to propose imaging features that can be replicated based on various MR pre-processing, contrasts, and scanning equipment. Automatically computing detailed LCNN features make it easy to analyze the relative properties of tumor and their classes for survival prediction, as we have done in our experiments.

Our combined feature method produced better performance and accurately measured the survival days on two different medical imaging datasets. It could be because combining many features into a single feature led to generalizability that is derived via integrated inference skills shared across numerous feature sets.

As demonstrated in our experiments, the features proposed in our paper readily generalize across different datasets like BraTS 2020 and Hecktor 2021. The proposed approach produced an excellent performance in the Hecktor 2021 dataset within the same feature set. However, BraTS, it did not outperform that well. However, one possible reason could be the BraTS20 dataset consisted of anaplastic astrocytomas, glioblastoma, or both that have various survival characteristics. The circumstance that BraTS20 has pre-operative that may play an essential role as well as the influences of surgery cannot be considered.

In this work, the focus is to extract radiomics features from the tumor region itself and the rest of the brain. We analyzed that the skewness, and kurtosis of deformation field amplitudes around the tumor together with conventional clinical and deep learning-based auto-generated features significantly improve survival models. Future work may, therefore, explore transformer-based deep learning methods along with radiomic features to further improve model accuracy. Since the transformers adopt the mechanism of self-attention, differentially weighing the significance of each part of the input data.

4 | CONCLUSION

In this paper, we have proposed a hybrid deep learning and radiomics-based method for survival days prediction of brain tumor patients. Further, the proposed hybrid solution is validated on the Hecktor2021 dataset for head and neck tumor segmentation to compare and substantiate the performance of our proposed approach. A variety of classical machine learning models have been trained using several sets of extracted imaging features while achieving better performance with the combined imaging features with non-imaging (Age) features. We proposed

various regressor methods for survival days prediction with a combined feature fusion approach. The features are extracted from deep learning and classical feature extraction techniques. We have also presented the explainability of the given set of features. It has been observed that combined radiomics and deep features can also have strong interpretability and clinical applicability for survival days prediction in brain tumors. The results have been compared with state-of-the-art methods and our proposed solution achieved excellent performance as compared to existing methods.

In the future, transformer and generative learning-based deep learning models will be explored to further improve the performance of the proposed approach for survival days prediction in brain tumor prognosis. We will compare foundation models with self-supervised techniques to further compare the performance of the proposed solution. We can train the model on other brain tumor datasets and validate with a few shots self-supervised methods.

AUTHOR CONTRIBUTIONS

Moona Mazher designed the model, analyzed the data, carried out the implementation, and wrote the manuscript. Abdul Qayyum and Mohamed Abdel-Nasser provided the general idea for this research work. Abdul Qayyum, Domenec Puig, and Mohammad Abdel-Nasser shared critical analysis and suggestions for the experiment and manuscript revision.

ACKNOWLEDGMENTS

This research work is supported by the Spanish Government through Projects TED2021-130081B-C21, PDC2022-133383-I00, PID2019-105789RB-I00.

CONFLICT OF INTEREST STATEMENT

The authors declare that there is no conflict of interest regarding the publication of this article.

DATA AVAILABILITY STATEMENT

The data that support the findings of this study are openly available in <https://www.med.upenn.edu/cbica/brats2020/data.html> at <https://www.med.upenn.edu/cbica/brats2020/data.html>.

ORCID

Moona Mazher  <https://orcid.org/0000-0003-4444-5776>

REFERENCES

- Castells X, García-Gómez JM, Navarro A, et al. Automated brain tumor biopsy prediction using single-labeling cDNA microarrays-based gene expression profiling. *Diagn Mol Pathol*. 2009;18(4):206-218. doi:10.1097/PDM.0b013e31818f071b
- Furnari FB, Fenton T, Bachoo RM, et al. Malignant astrocytic glioma: genetics, biology, and paths to treatment. *Genes Dev*. 2007;21(21):2683-2710. doi:10.1101/gad.1596707
- Louis DN, Ohgaki H, Wiestler OD, et al. The 2007 WHO classification of Tumours of the central nervous system. *Acta Neuropathol*. 2007;114(2):97-109. doi:10.1007/s00401-007-0243-4
- Chaddad A, Kucharczyk MJ, Daniel P, et al. Radiomics in glioblastoma: current status and challenges facing clinical implementation. *Front Oncol*. 2019;9:374. doi:10.3389/fonc.2019.00374
- Almalki YE, Qayyum A, Irfan M, et al. A novel method for COVID-19 diagnosis using artificial intelligence in chest X-ray images. *Healthcare*. 2021;9(5):522. doi:10.3390/healthcare9050522
- Seow P, Wong JHD, Ahmad-Annuar A, Mahajan A, Abdullah NA, Ramli N. Quantitative magnetic resonance imaging and radiogenomic biomarkers for glioma characterisation: a systematic review. *Br J Radiol*. 2018;91(1092):20170930. doi:10.1259/bjr.20170930
- Yao J, Wang S, Zhu X, Huang J. Imaging biomarker discovery for lung cancer survival prediction. In *Medical Image Computing and Computer-Assisted Intervention—MICCAI, 19th International Conference, Athens, Greece, 17-21 October 2016*. Springer International Publishing; 2016.
- Coroller TP, Grossmann P, Hou Y, et al. CT-based radiomic signature predicts distant metastasis in lung adenocarcinoma. *Radiother Oncol*. 2015;114(3):345-350. doi:10.1016/j.radonc.2015.02.015
- Shboul ZA, Alam M, Vidyaratne L, Pei L, Elbakary MI, Iftekharruddin KM. Feature-guided deep radiomics for glioblastoma patient survival prediction. *Front Neurosci*. 2019;13:966. doi:10.3389/fnins.2019.00966
- Feng X, Tustison NJ, Patel SH, Meyer CH. Brain tumor segmentation using an ensemble of 3D U-nets and overall survival prediction using radiomic features. *Front Comput Neurosci*. 2020;14:25. doi:10.3389/fncom.2020.00025
- Osman AFI. A multi-parametric MRI-based radiomics signature and a practical ML model for stratifying glioblastoma patients based on survival toward precision oncology. *Front Comput Neurosci*. 2019;13:58. doi:10.3389/fncom.2019.00058
- Sun L, Zhang S, Chen H, Luo L. Brain tumor segmentation and survival prediction using multimodal MRI scans with deep learning. *Front Neurosci*. 2019;13:810. doi:10.3389/fnins.2019.00810
- Baid U, Shah NA, Talbar S. Brain tumor segmentation with cascaded deep convolutional neural network. In *Brainlesion: Glioma, Multiple Sclerosis, Stroke and Traumatic Brain Injuries: 5th International Workshop, BrainLes 2019, Held in Conjunction with MICCAI, Shenzhen, China, 17 October 2019*. Springer International Publishing; 2020.
- Baid U, Talbar S, Rane S, Gupta S, Thakur MH, Moiyadi A, Mahajan A. Deep learning radiomics algorithm for gliomas (drag) model: a novel approach using 3d unet based deep convolutional neural network for predicting survival in gliomas. In *Brainlesion: Glioma, Multiple Sclerosis, Stroke and Traumatic Brain Injuries: 4th International Workshop, BrainLes, Held in Conjunction with MICCAI, Granada, Spain, 16 September 2018*. Springer International Publishing; 2019.
- Weninger L, Haarbuerger C, Merhof D. Robustness of radiomics for survival prediction of brain tumor patients depending on

- resection status. *Front Comput Neurosci.* 2019;13:73. doi:10.3389/fncom.2019.00073
16. Bae S, Choi YS, Ahn SS, et al. Radiomic MRI phenotyping of glioblastoma: improving survival prediction. *Radiology.* 2018; 289(3):797-806. doi:10.1148/radiol.2018180200
 17. Noreen N, Palaniappan S, Qayyum A, Ahmad I, Imran M, Shoaib M. A deep learning model based on concatenation approach for the diagnosis of brain tumor. *IEEE Access.* 2020;8: 55135-55144. doi:10.1109/ACCESS.2020.2978629
 18. Payette K, Li H, de Dumast P, et al. Fetal brain tissue annotation and segmentation challenge results. 2022 [Online]. <http://arxiv.org/abs/2204.09573>
 19. Lalande A, Chen Z, Pommier T, et al. Deep learning methods for automatic evaluation of delayed enhancement-MRI. The results of the EMIDEC challenge. *Med Image Anal.* 2022;79: 102428. doi:10.1016/j.media.2022.102428
 20. Bano S, Casella A, Vasconcelos F, et al. FetReg2021: a challenge on placental vessel segmentation and registration in fetoscopy. 2022. doi:10.48550/arXiv:2206.12512
 21. de Vente C, Vermeer KA, Jaccard N, et al. AIROGS: artificial intelligence for RObusT glaucoma screening challenge. 2023 doi:10.1109/TMI.2023.3313786
 22. Li X, Luo G, Wang K, et al. The state-of-the-art 3D anisotropic intracranial hemorrhage segmentation on non-contrast head CT: the INSTANCE challenge. 2023 [Online]. <http://arxiv.org/abs/2301.03281>
 23. Iqbal S, Ghani Khan MU, Saba T, et al. Deep learning model integrating features and novel classifiers fusion for brain tumor segmentation," *Microsc Res Tech.* 2019;82(8):1302-1315. doi:10.1002/jemt.23281
 24. Banerjee S, Mitra S, Shankar BU. Multi-planar spatial-ConvNet for segmentation and survival prediction in brain cancer. In *Brainlesion: Glioma, Multiple Sclerosis, Stroke and Traumatic Brain Injuries: 4th International Workshop, BrainLes, Held in Conjunction with MICCAI, Granada, Spain, 16 September 2018.* Springer International Publishing; 2019.
 25. Jungo A, McKinley R, Meier R, Knecht U, Vera L, Pérez-Beteta J, Reyes M. Towards uncertainty-assisted brain tumor segmentation and survival prediction. In *Brainlesion: Glioma, Multiple Sclerosis, Stroke and Traumatic Brain Injuries: Third International Workshop, BrainLes, Held in Conjunction with MICCAI, Quebec City, QC, Canada, 14 September 2017.* Springer International Publishing; 2018.
 26. Islam M, Vs V, Jose VJM, Wijethilake N, Utkarsh U, Ren H. Brain tumor segmentation and survival prediction using 3D attention UNet. 2021 [Online]. <http://arxiv.org/abs/2104.00985>
 27. Huang H, Zhang W, Fang Y, Hong J, Su S, Lai X. Overall survival prediction for gliomas using a novel compound approach. *Front Oncol.* 2021;11:724191. doi:10.3389/fonc.2021.724191
 28. Pálsson S, Cerri S, Poulsen HS, Urup T, Law I, Van Leemput K. Predicting survival of glioblastoma from automatic whole-brain and tumor segmentation of MR images. *Sci Rep.* 2022;12(1): 19744. doi:10.1038/s41598-022-19223-3
 29. Menze BH, Jakab A, Bauer S, et al. The multimodal brain tumor image segmentation benchmark (BRATS). *IEEE Trans Med Imaging.* 2015;34(10):1993-2024. doi:10.1109/TMI.2014.2377694
 30. Mazher M, Qayyum A, Puig D, Abdel-Nasser M. Effective approaches to fetal brain segmentation in MRI and gestational age estimation by utilizing a multiview deep inception residual network and radiomics. *Entropy.* 2022;24(12):1708. doi:10.3390/e24121708
 31. Taghanaki SA, Zheng Y, Kevin Zhou S, et al. Combo loss: handling input and output imbalance in multi-organ segmentation. *Comput Med Imaging Graph.* 2019;75:24-33. doi:10.1016/j.compedimag.2019.04.005
 32. Hussain S, Haider S, Maqsood S, Damaševičius R, Maskeliūnas R, Khan M. ETISTP: an enhanced model for brain tumor identification and survival time prediction. *Diagnostics.* 2023;13(8):1456.
 33. Bourigault E, McGowan DR, Mehranian A, Papież BW. Multimodal PET/CT tumour segmentation and prediction of progression-free survival using a full-scale UNet with attention. 2021 [Online]. <http://arxiv.org/abs/2111.03848>
 34. Juanco-Müller ÁV, Mota JFC, Goatman K, Hoogendoorn C. Deep supervoxel segmentation for survival analysis in head and neck cancer patients. In *3D Head and Neck Tumor Segmentation in PET/CT Challenge.* Springer International Publishing; 2021.
 35. Starke S, Leger S, Zwanenburg A, et al. 2D and 3D convolutional neural networks for outcome modelling of locally advanced head and neck squamous cell carcinoma. *Sci Rep.* 2020;10(1):15625. doi:10.1038/s41598-020-70542-9
 36. Qayyum A, Mazher M, Khan T, Razzak I. Semi-supervised 3D-InceptionNet for segmentation and survival prediction of head and neck primary cancers. *Eng Appl Artif Intel.* 2023; 117:105590.
 37. Eisenmann M, Reinke A, Weru V, et al. Biomedical image analysis competitions: the state of current participation practice. *arXiv Preprint arXiv:2212.08568.* 2022.
 38. Qayyum A, Mazhar M, Razzak I, Bouadjenek MR. Multilevel depth-wise context attention network with atrous mechanism for segmentation of COVID19 affected regions. *Neural Comput Appl.* 2021;35:1-13.

How to cite this article: Mazher M, Qayyum A, Puig D, Abdel-Nasser M. Deep learning-based survival prediction of brain tumor patients using attention-guided 3D convolutional neural network with radiomics approach from multimodality magnetic resonance imaging. *Int J Imaging Syst Technol.* 2024;34(1):e23010. doi:10.1002/ima.23010